

# Manual: Code SHARM (SHARM-Mie)

Alexei Lyapustin UMBC GEST/NASA GSFC

NASA Goddard Space Flight Center, Mail Code 614.4, Greenbelt, MD 20771

alyapust@pop900.gsfc.nasa.gov

## 1. Overview

SHARM is a new 1-D radiative transfer (RT) code designed to compute monochromatic radiance/flux in the shortwave spectral region over a Lambertian or anisotropic surface. The atmospheric properties can change arbitrarily in the vertical dimension. The algorithm uses the method of spherical harmonics (MSH) [Muldasev *et al.*, 1998; Lyapustin and Muldasev, 1999, 2000] with the boundary conditions in the form of Marshak [1947]. The code is rigorous in a sense that its solution converges to the true value at increase of the order of MSH. Two numerical “tricks” implemented in Sharm-1D make this code very fast. The first one uses special symmetry properties of the matrix of MSH system to reduce its size by a factor of two for the subsequent singular value decomposition (SVD), which was originally suggested for MSH by Karp *et al.* [1980]. The second one is an innovative “*correction function*” method of angular smoothing of solution developed by Dr. Muldasev. This method yields a high accuracy at relatively low orders of MSH [Muldasev *et al.*, 1998] and is faster than the “source function method” [Dave and Armstrong, 1974]. A recently performed intercomparison among several 1-D codes [Lyapustin, 2002] showed that in the test cases Sharm-1D was as accurate as DISORT [Stamnes *et al.*, 1988], yet faster in calculations with aerosol phase functions. On the other hand, the new code has yet to accumulate a long history of testing in the most “adverse” conditions that DISORT has. Therefore, it is advisable to the users to validate the results of Sharm-1D calculations against DISORT in the most difficult cases, at least initially.

### Limitations:

- Plane-parallel geometry;
- Monochromatic;
- Unpolarized;
- Radiance and fluxes are calculated only on the interfaces of atmospheric layers.

### Main Features:

- Calculations for multiple wavelengths in one run;
- Simultaneous calculations for multiple SZA, VZA, and view azimuths;
- Lambertian or anisotropic surface reflectance. In anisotropic case, the land surface reflectance can be described by either RPV/MRPV model [Rahman *et al.*, 1993] (see sec. 6.3.1) or Li Sparse-Ross Thick (LSRT) linear kernel model [Lucht *et al.*, 2000]. Over the ocean, the reflectance of roughened water surface is modeled by either azimuthally independent model of Nakajima and Tanaka (NT), [1983] or azimuth-dependent Cox and Munk [1954] model (CoxMunk) with the wave mutual shadowing (see sec. 6.3.3). The water refractive index in the 0.3-2.4  $\mu\text{m}$  region is tabulated based on Hale and Querry [1973]. The azimuthally independent case is solved rigorously. The asymmetric case is solved approximately: the direct-beam reflected radiance is calculated with asymmetric CoxMunk, and the diffuse surface-reflected term is calculated with azimuthally independent NT model.
- The code is written in C language with C++ features.

### History:

The original code with the Lambertian boundary was developed in far nineties by Dr. Tolegen Muldashev who worked for Space Research Institute, Kazakstan Academy of Sciences. He also suggested the name, SHARM. Later, this talented mathematician made a successful career in busyness. I contributed to this code by developing the boundary conditions and “correction function” method for anisotropic reflectance, and improving stability of the code.

**Copywrite:** *Codes Phase, SHARM, SHARM-Mie have a NASA copywrite.*

Academic users: The unmodified version of code SHARM can be freely distributed and used in research and teaching. It may not be sold, or distributed on commercial basis.

Commercial and other users: Use of this code in commercial applications is forbidden without a written approval of the author.

### Disclaimer:

Authors of this code are not responsible for the consequences resulting from improper use or modification of this code. Control of accuracy of the results is the sole responsibility of the user.

## 2. Main Definitions

The MSH algorithm uses the plane-parallel model of the atmosphere that is divided into  $N$  homogeneous layers (Figure 1). Each layer  $n$  is characterized by its optical thickness  $\Delta\tau_n = \tau_n - \tau_{n-1}$ , single scattering albedo  $\omega_n$ , and scattering function  $\chi_n(\gamma)$ . The optical thickness and number of layer are counted from the top of the atmosphere (TOA), in opposite to the altitude.

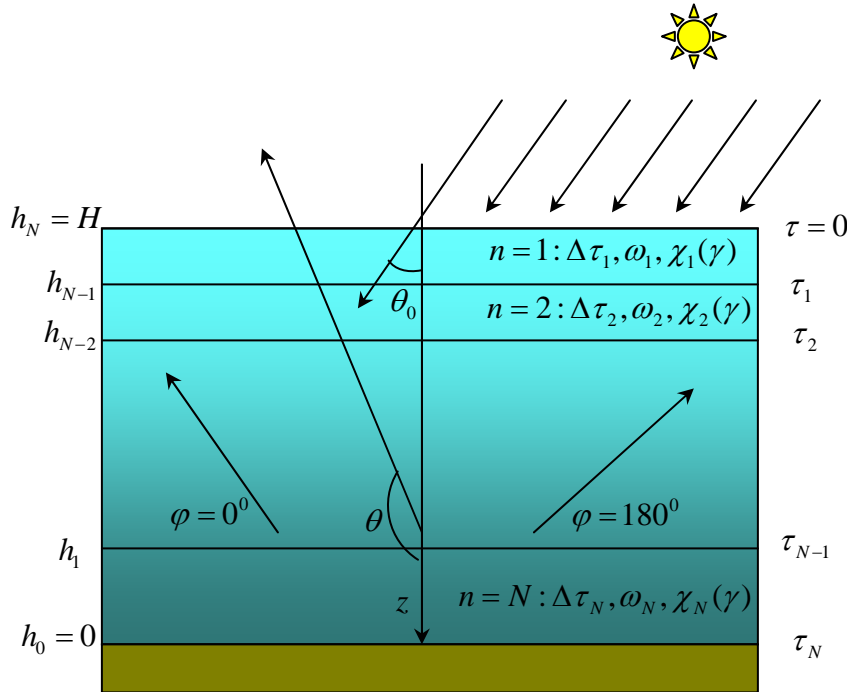


Figure 1.

In the accepted system of coordinates, z-axis is directed downward. For this reason, solar zenith angle (SZA) changes from 0 to 90°, and view zenith angle (VZA) changes in the ranges 90-180° ( $\mu < 0$ ) for upward directions (satellite view geometry), and 0-90° ( $\mu > 0$ ) for downward directions (ground – based observations of sky). Figure 1 shows the relative azimuth for observations in the principle plane  $\varphi = 0^\circ$  and  $\varphi = 180^\circ$ .

### 3. Expansion of Scattering Function

Code SHARM comes in package with code PHASE which calculates Legendre polynomial expansion of the scattering function “\*.dat”. It creates the file “\*.ph” that is required to run the main program Sharm-1D. The scattering function should be prepared in the file “\*.dat” (e.g. “phase1.dat”) in the following format:

1. N\_wavln, N\_angles      the number of wavelengths, for which scattering function is given, and the number of angular nodes of phase function
2.  $\gamma_i, \{ \chi(\gamma_i)_k, k=1, \dots, N\_wavln \}$  (in line: angle, and phase function values for a given angle for all wavelengths)

Example:

	7	93						
.0	.1499E+03	.7550E+02	.4114E+02	.1323E+02	.3201E+01	.1130E+01	.4382E+00	
1.0	.9676E+02	.5278E+02	.3071E+02	.1097E+02	.2905E+01	.1069E+01	.4244E+00	
...								
179.0	.4418E+00	.2693E+00	.1784E+00	.8164E-01	.2494E-01	.8858E-02	.3291E-02	
180.0	.4466E+00	.2724E+00	.1805E+00	.8260E-01	.2524E-01	.8975E-02	.3336E-02	

The format of floating point numbers is arbitrary, non necessarily ‘E’. The program will ask for the name of file with the scattering function. For the above example, you can enter either *phase1*, or *phase1.dat*. The result (expansion coefficients, and nodes and coefficients of the rational polynomial interpolation that are required for code SHARM) is recorded in file “\*.ph” (in the above example, “*phase1.ph*”). The scattering function is normalized internally, so the user does not need to care about normalization of the scattering function.

The user should compile the file *phase.cpp* as a main program. Currently, the order of Lobatto quadrature used for expansion is set to a high value ( $nlob=901$ ), so it should work satisfactorily for practically all cases.

I recommend to keep the files with aerosol phase functions and the results of their expansion in the separate directory (of program *phase.cpp*). Since the user usually accumulates a large number of different aerosol or cloud phase functions, this separation would create less havoc in the work directory of the main program SHARM. The path to the phase functions is one of the input parameters for SHARM (see below).

THE EXPANSION OF AEROSOL PHASE FUNCTION SHOULD BE DONE **BEFORE** YOU RUN SHARM!!!

### 4. Input data

The input data are arranged in three files:

- *Configuration file (config.par)*: defines wavelengths, order of the MSH, the incidence-view geometry, the names of input atmospheric and surface properties files, and governs printing of the results;
- *Atmospheric Properties file (\*.atm)*: describes parameters of the atmosphere;
- *Surface Properties file (\*.sfc)*: describes surface reflectance.

## 4.1 Configuration/Geometry File (config.par)

### 1. MonoChrom

This line states that calculations will be performed in a monochromatic mode (currently not used). In future version, I will add broadband capabilities, and this line will be used to discriminate between calculations with different spectral resolution.

### 2. N\_wavln, wavln[0], wavln[1], ..., wavln[N\_wavln-1]

the number of wavelengths, and wavelengths in  $\mu\text{m}$ ;

### 3. nb the order of MSH. Must be *even*;

### 4. ks, cs0gr[0], cs0gr[1], ..., cs0gr[ks-1]

number of SZA, and solar zenith angles (in degrees:  $0 \leq \theta_0 < 90^\circ$ );

### 5. mm, chVZAinputType, tp[0], tp[1], ..., tp[mm-1] mm - number of VZA, tp[] - cosines of VZA (<0 for upward directions);

*char* chVZAinputType describes spacing of VZA points (used to reduce input). It takes values of: 'p' – individual points, and 'e' - equidistant. If (chVZAinputType = 'p'), user must provide all *mm* values, tp[0], ..., tp[mm-1]. When the number of view angles is large (e.g.100), and user needs to know the angular trend rather than radiances at specific angles, the equidistant mode 'e' can be used. It provides the equidistant spacing between the cosines of VZA. In this case, the first tp[0] and the last tp[mm-1] points should be specified, and all of the intermediary points are calculated automatically.

**Examples:** A) 5 p -0.233 -0.785 -0.989 0.432 0.99345 B) 41 e -0.2 -1. The case B) is given for the upward directions (tp[]<0).

### 6. naz, az[0], az[1], ..., az[naz-1] number of azimuthal angles, and relative azimuths;

### 7. FileName of Atmospheric Properties (\*.atm) input file.

### 8. FileName of Surface Properties (\*.sfc) input file.

### 9. FileName and Access Mode of the output file.

An Access Mode follows the c standard:

w new file will be created. If the file FileName exists, it will be deleted first.

a+ results will be written at the end of the file FileName. If the file FileName does not exist, it will be created first.

### 10. Print Mode.

Two print parameters govern the output of radiance and fluxes:

#### 1. szPrint - specifies interfaces for which results are printed. It can be one of three:

BOA - print for BOA (bottom of the atmosphere);

TOA - print for TOA;

ALL - print for all interfaces;

#### 2. szRTMode - specifies what to calculate and print. It can be one of three:

RadOnly - print radiance only;

FluxOnly - print/calculate fluxes only;

FluxRad - prints both radiances and fluxes.

EXAMPLE (file “config.par”)	Line number
MonoChrom	( 1 )
2 0.412 2.13	( 2 )
32	( 3 )
3 30. 45. 60.	( 4 )
9 e -0.2 -1.	( 5 )
4 0. 45. 90. 180.	( 6 )
1-3.atm	( 7 )
1.sfc	( 8 )
radiance.dat w	( 9 )
TOA FluxRad	( 10 )

## 4.2 Atmospheric Properties File (\*.atm)

1. szAtmType one of 6 Standard Models of the Atmosphere from Lowtran/Modtran: "Tropical", "Midlatitude Summer", "Midlatitude Winter", "Sub-Arctic Summer", "Sub-Arctic Winter", "1976 US Standard". Defines vertical profiles of atmospheric pressure and temperature (file “profile.h”)
2. ib number of layers in atmosphere (starting from the TOA).
3. height[0], ..., height[ib] altitude of boundaries of ib layers (in km) starting from TOA, e.g. height[0]=100 km (TOA) & height[ib]=0 (BOA).
4. Next, sequentially for each wavelength {  
 $\Delta \tau^a [1], \dots, \Delta \tau^a [ib]$  aerosol optical thickness of ib layers {  $\Delta \tau_i^a = \tau_i^a - \tau_{i-1}^a$ , where  $\tau_{i=0}^a = 0$ ,  $\tau_{i=ib}^a = \tau_{total}^a$  }.  
 $\omega^a [0], \dots, \omega^a [ib-1]$  aerosol single scattering albedo of ib layers.  
 $\tau_{i=1}^{g-abs} [1], \dots, \tau_{i=ib}^{g-abs} [ib]$  optical thickness of gaseous absorption on the boundaries of layers (  $\tau_{i=1}^{g-abs}, \dots, \tau_{i=ib}^{g-abs}$  . By default,  $\tau_{i=0}^{g-abs} = 0$  )  
}
5. szPhasePath path to a directory containing aerosol scattering functions, e.g. c:\\workDir\\Phase\\. For a current directory, specify “./” for unix, and “../” for windows systems.
6. phase[0], ..., phase[ib-1] names of files “\*.ph” containing Legendre expansion of aerosol scattering functions in ib layers. If the aerosol phase function is constant with altitude, specify the same filename \*.ph for all layers.  
Files “name.ph” are produced by a separate program phase.c from the file “name.dat” containing nodes (scattering angles) and values of the aerosol scattering function (see sec.3).
7. szDeltaM Specifies whether or not to use the DeltaM method. Takes value of DeltaM\_NO or DeltaM\_YES. In most cases (calculations for aerosol atmospheres), DeltaM method should NOT be used (DeltaM\_NO). It should be used though when the phase function is very asymmetric (e.g. clouds, or coarse-particle dust).

EXAMPLE (file “3layers.atm”)	Line number
(the word “Comment” and the following line of text is for explanation only and should NOT be in the file)	
1976 US Standard	( 1 )
3	( 2 )
40. 10. 2. 0.	( 3 )

Comment :

$$\Delta \tau_1^a \quad \Delta \tau_2^a \quad \Delta \tau_3^a \quad \omega_0^a \quad \omega_1^a \quad \omega_2^a \quad \tau_1^{g-abs} \quad \tau_2^{g-abs} \quad \tau_3^{g-abs} \quad (4)$$

```
0.0169 0.0506 0.2696      0.9748 0.9522 0.9286      0.0      0.0      0.0
0.0011 0.0032 0.0170      0.9364 0.9297 0.9110      0.03     0.01     0.003
```

Comment: Above, the first line is for wavelength 0.412  $\mu\text{m}$ , and second one is for 2.13  $\mu\text{m}$ .

```
c:\workDir\Phase\
phase_01.ph  phase_02.ph  phase_03.ph
DeltaM_NO
```

(5)  
(6)  
(7)

### 4.3 Surface Properties Files (\*.sfc)

1. chLambert                      Type of surface reflectance. Takes values of 'L' – Lambertian, or 'A' – anisotropic.  
The subsequent records of surface properties file differ depending on the type of reflectance.  
*If the reflectance is Lambertian:*
2. q [0], ...q[N\_wavln-1]              Surface albedo at N\_wavln wavelengths.

EXAMPLE (file "1.sfc" for Lambertian surface, two wavelengths)              Line number

```
L
0.033 0.25
```

(1)  
(2)

*If the reflectance is anisotropic, then user should specify:*

2. szBRDFtype                      Parametric Model of BRF used. Takes values of:  
RPV (land, RPV model),  
MRPV (land, MRPV model),  
LSRT (land, LSRT model), or  
NT (ocean, isotropic/azimuthally independent NT model after *Nakajima and Tanaka*, 1983),  
CoxMunk (ocean, full anisotropic Cox-Munk model with Gram-Charlier expansion).

Over land, specify three parameters of the BRF model for each wavelength.

3.  $\rho_0, k, \alpha$  (if szBRDFtype="RPV"),  
 $\rho_0, k, b$  (if szBRDFtype= "MRPV"), or  
 $w_L, w_v, w_{go}$  (if szBRDFtype= "LSRT").

EXAMPLE (file "1A.sfc" for non-Lambertian surface, two wavelengths)              Line number

```
A
RPV
0.017 0.630 -0.169
0.039 0.810 -0.169
```

(1)  
(2)  
(3)

If szBRDFtype="NT" or "CoxMunk", specify the wind speed in m/s, and a relative azimuth of wind direction with respect to principal plane ( $\Delta\varphi_w = \varphi_{Wind} - \varphi_0$ ). The azimuth is counted clock-wise from the North. The value  $\Delta\varphi_w$  is not used when calculations are performed with azimuthally-independent NT model, however some arbitrary number still should be specified (e.g.  $\Delta\varphi_w=0$ ).

3. wind\_speed,  $\Delta\varphi_w$

EXAMPLE (file “1A.sfc” for water surface, wind speed of 11 m/s, and  $\Delta\phi_w=30^\circ$ ).

A (1)  
 NT (2)  
 11. 30. (3)

## 5. Accuracy and Convergence

Generally, the higher asymmetry of the phase function, the higher order of solution is required to achieve a given accuracy. For typical continental/marine aerosols (excluding dust and clouds), I recommend using  $nb=24-36$ . These orders guarantee the relative accuracy of radiance calculations of better than 0.2-0.3% for the range of view/solar zenith angles of 0-80°. The value of  $nb=128$  ensures the accuracy of  $\approx 0.02\%$ . In any case, please check the accuracy of your calculations with selected  $nb$  against, say,  $nb=128$ .

The convergence slows with the increase of view/solar zenith angle. Therefore, the rule of thumb is to use higher orders  $nb$  if you have high solar or view zenith angles to achieve the same level of accuracy.

In case of highly asymmetric phase functions with strong forward scattering peak (clouds), the order of  $nb=128$  gives the accuracy of about or better than 0.5-1%, and  $nb=256$  would provide an accuracy of about or better than 0.2% (as compared to the solution at  $nb=512$ ). To improve convergence of Sharm-1D in these cases I added Delta-M method.

The calculations of fluxes require considerably smaller orders of MSH. For the flux-only calculations, using  $nb=12-24$  will be sufficient for most applications.

**Rem.** The suggested orders of MSH **nb** are for the radiance calculations. If only fluxes are required, one can use considerably lower values of **nb**.

## 6. Built-in Models

### 6.1 Molecular Scattering

- The scattering function of air is considered to be purely Rayleigh. A slight asymmetry caused by depolarization is ignored in this version.
- The vertical profile of molecular optical thickness is calculated as:

$$\tau^m(\lambda, z) = \int_0^z \sigma(\lambda, z') N(z') dz',$$

where  $\sigma$  is a Rayleigh scattering cross section per molecule,  $N(z) = N_s \frac{P(z)}{P_s} \frac{T_s}{T(z)}$  is a concentration of air molecules at altitude  $z$ , and  $P_s = 1013.25 \text{ mb}$ ,  $T_s = 273.15 \text{ K}$  are the standard pressure and temperature. The vertical profile of pressure and temperature can be selected from six standard atmospheric profiles (Tropical, Midlatitude Summer, Midlatitude Winter, SubArctic Summer, SubArctic Winter, 1976 US Standard). The integral over altitude is evaluated with the gaussian quadrature.

The Rayleigh scattering cross section is calculated with the algorithm of *Bodhain et al.* [1999], which has a uniformly high accuracy across the spectral range from UV to the shortwave IR.

## 6.2 Gaseous Absorption

Gaseous absorption is NOT automatically incorporated in this version. I am working on merging the IPC (Interpolation and Profile Correction) method [*Lyapustin*, 2003] with SHARM-1D code for the visible and shortwave-IR spectrum using the HITRAN-2000 [*Rothman et al.*, 2002] spectral database. The IPC method will allow fast and accurate RT calculations with an arbitrary spectral resolution, including monochromatic mode. In the meantime, SHARM accommodates user-supplied gaseous absorption via gaseous absorption optical thickness ( $\tau_i^{g-abs}$ ) in the file of atmospheric properties.

## 6.3 Models of BRF

### 6.3.1 RPV model

This model depends on three parameters ( $\rho_0, k, \alpha$ ):

The RPV model depends on three parameters ( $\rho_0, k, \alpha$ ):

$$\rho(\mu_0; -\mu; \varphi) = \rho_0 M(k) F(\alpha) H(\rho_0), \quad (L-1)$$

$$M(k) = [\mu\mu_0(\mu + \mu_0)]^{k-1}, \quad F(\alpha) = \frac{1 - \alpha^2}{[1 - 2\alpha \cos \gamma + \alpha^2]^{3/2}}, \quad H(\rho_0) = \left\{1 + \frac{1 - \rho_0}{1 + G}\right\}, \quad (L-2)$$

where  $\gamma$  is angle of scattering,

$$\cos \gamma = -\mu_0\mu + \sqrt{1 - \mu_0^2} \sqrt{1 - \mu^2} \cos(\varphi - \varphi_0), \quad (L-3)$$

and

$$G = \sqrt{tg^2\theta_0 + tg^2\theta + 2tg\theta_0tg\theta \cos(\varphi - \varphi_0)}. \quad (L-4)$$

Note that the hot spot lies in the direction of backscattering,  $\varphi - \varphi_0 = \pi$ .

- Usually, the Minnaert's exponent  $k$  is less than 1. It means that at small values of  $\mu, \mu_0$ , the total BRF may become unphysically large, and albedo at low SZA may exceed 1. As a remedy, I introduced an artificial threshold on the values of BRF at high angles. This threshold has a form: if ( $|\mu| < 0.03$ )  $BRF(\mu) = BRF(0.03)$  (the same for  $\mu_0$ ).

- For user's convenience, Table 1 provides some of the best fit RPV parameters for different land covers [*Engelsen et al.*, 1996].

**Table 1.** Best Fit Parameters ( $\rho$ ,  $k$ ,  $\alpha$ ) of the RPV Model for different Land Covers

$N$	Surface	$r$	$\rho$	$\alpha$	$k$	$r$	$\rho$	$\alpha$	$k$
		Visible				near-IR			
1	Spruce	0.971	0.008	-0.308	0.554	0.952	0.050	-0.201	0.581
2	sparse erectophile	0.967	0.064	-0.001	1.207	0.971	0.278	-0.006	0.725
3	tropical forest	0.977	0.012	-0.169	0.651	0.986	0.303	-0.034	0.729
4	Plowed field	0.975	0.072	-0.257	0.668	0.976	0.077	-0.252	0.678
5	Grasses	0.958	0.014	-0.169	0.810	0.981	0.242	-0.032	0.637
6	Broad leaf crops	0.954	0.012	-0.281	0.742	0.975	0.204	-0.089	0.658
7	Savannah	0.960	0.010	-0.287	0.463	0.953	0.219	-0.050	0.673
8	leaf forest	0.980	0.022	-0.228	0.633	0.981	0.285	-0.060	0.745
9	Conifers	0.978	0.018	-0.282	0.364	0.964	0.235	-0.095	0.758
10	hardwood forest winter	0.974	0.028	-0.175	0.768	0.950	0.066	-0.141	0.735
11	loam soil	0.958	0.147	-0.096	0.839	0.952	0.195	-0.097	0.850
12	irrigated wheat	0.965	0.027	-0.078	0.382	0.951	0.306	-0.008	0.606

**Parameter  $r$  is the correlation coefficient between the original BRF data (experimental or theoretical) and the RPV model.**

### 6.3.2 MRPV model

In the *MRPV* model, the term  $F(\alpha)$  is substituted by  $F(\alpha) = \exp(\alpha \times \cos \gamma)$ . This modification yields a nearly linear expression for the model parameters after logarithmic transformation [Martonchik et al., 1998].

### 6.3.3 Land: Linear LSRT model

This model is represented by a sum of Lambertian, geometric-optics and volume scattering terms:

$$\rho(\mu_0, -\mu, \varphi) = k_L + k_{go} f_{go}(\mu_0, \mu, \varphi) + k_v f_v(\mu_0, \mu, \varphi). \quad (L-5)$$

The kernel functions are given by the following expressions:

$$f_v = \frac{(\frac{\pi}{2} - \gamma) \cos \gamma + \sin \gamma}{\mu_0 + \mu} - \frac{\pi}{4}, \quad (L-6)$$

$$f_{go} = O(\mu_0, \mu, \varphi) - \mu'^{-1} - \mu_0'^{-1} + \frac{1}{2}(1 + \cos \gamma') \mu'^{-1} \mu_0'^{-1}, \quad (L-7)$$

where

$$O(\mu_0, \mu, \varphi) = \frac{1}{\pi} (t - \sin t \cos t) (|\mu'|^{-1} + \mu_0'^{-1}), \quad (L-8)$$

$$\cos t = \frac{h \sqrt{(G')^2 + (tg \theta'_0 tg \theta' \sin(\varphi - \varphi_0))^2}}{b |\mu'|^{-1} + \mu_0'^{-1}}, \text{ with a constraint } |\cos t| \leq 1. \quad (L-9)$$

The primed angles ( $\theta'_0$ ,  $\theta'$ ) are obtained by scaling  $tg\theta' = \frac{b}{r}tg\theta$ . Note that  $\cos\gamma'$  in (L-7) and  $G'$  in (L-9) are calculated for primed angles ( $\theta'_0$ ,  $\theta'$ ) using equations (L-3) and (L-4), respectively.

The ratio of structural parameters is fixed ( $h/b=2$  and  $b/r = 1$ ) [Lucht et al., 2000]. Thus, the functions  $f_v$ ,  $f_{go}$  depend on angles only, and BRF is defined by three coefficients  $\{k_L, k_{go}, k_v\}$ .

One should exercise caution with this model at high zenith angles larger than  $80^\circ$ , when the BRF may become negative or, in the contrary, grow very fast [Gao et al., 2000].

#### 6.3.4 Model of Ocean Reflectance

General Comment: Below, only the Fresnel reflectance from the water surface is considered, and the water-leaving radiance is set to zero.

The lower boundary condition for the radiance reflected from the water surface is written as follows:

$$I^\uparrow(\mu, \varphi) = \pi S_\lambda e^{-\frac{\tau}{\mu_0}} R(\mu_0, \mu, \varphi - \varphi_0) + \int_{\Omega^+} I^\downarrow(\mu', \varphi') R(\mu', \mu, \varphi - \varphi') d\mu' d\varphi'.$$

##### 6.3.4.1 Azimuthally-Independent Model (NT)

Following Nakajima and Tanaka [1983], the reflection coefficient can be expressed as:

$$R(\mu', \mu, \varphi - \varphi') = \frac{1}{4\mu\mu_n} R^{Fr}(\chi) P(\mu_n) S(\mu', \mu), \quad (O-1)$$

where Fresnel reflectance for unpolarized radiance is

$$R^{Fr} = \frac{1}{2} \{r_\parallel^2 + r_\perp^2\}, \quad r_\parallel = \frac{\sqrt{m^2 - \sin^2 \theta_i} - m^2 \cos \theta_i}{\sqrt{m^2 - \sin^2 \theta_i} + m^2 \cos \theta_i}, \quad r_\perp = \frac{\cos \theta_i - \sqrt{m^2 - \sin^2 \theta_i}}{\cos \theta_i + \sqrt{m^2 - \sin^2 \theta_i}}.$$

Here,  $m = n + ik$  is complex refractive index, and  $\theta_i$  is angle of incidence ( $\mu' = \cos \theta_i$ ).  $\chi$  is the reflection angle from the facet with the normal  $\mu_n$ .

The probability density function of slope distribution is given by

$$P(\mu_n) = \frac{1}{\pi \sigma^2 \mu_n^3} \exp\left(-\frac{1 - \mu_n^2}{\sigma^2 \mu_n^2}\right). \quad (O-2)$$

where  $\sigma^2 = 0.00534u$  [Nakajima and Tanaka, 1983], and  $u$  [m/s] is wind speed 10 meters above the water surface.

Introducing  $a = \frac{1 + \cos 2\chi}{(\mu + \mu')^2}$ , where  $2\chi$  is reflection angle,  $\cos 2\chi = \mu\mu' - \sqrt{1 - \mu^2} \sqrt{1 - \mu'^2} \cos(\varphi - \varphi')$

(note that in the coordinate system accepted here  $\mu' > 0$ , and  $\mu < 0$ ), we can find [Gordon and Wang, 1992]:

$$\frac{1}{4\mu\mu_n} P(\mu_n) = \frac{1}{4\pi \sigma^2 \mu \mu_n^4} \exp\left(-\frac{1 - \mu_n^2}{\sigma^2 \mu_n^2}\right) = \frac{a^2}{\mu \pi \sigma^2} \exp\left(\frac{1 - 2a}{\sigma^2}\right).$$

Finally, the wave-shadowing factor is:

$$S(\mu', \mu) = \frac{1}{1 + F(g) + F(g')},$$

where  $g = \frac{\mu}{\sigma\sqrt{1-\mu^2}}$ , and

$$F(g) = \frac{1}{2} \left[ \frac{\exp(-g^2)}{g\sqrt{\pi}} - \frac{2}{\sqrt{\pi}} \int_g^\infty \exp(-t^2) dt \right] = \frac{\exp(-g^2)}{2g\sqrt{\pi}} - \frac{1}{2} + \Phi(\sqrt{2}g),$$

$$\Phi(\sqrt{2}g) = \frac{1}{\sqrt{2\pi}} \int_0^{\sqrt{2}g} \exp(-\frac{z^2}{2}) dz - \text{probability integral for the normal distribution (tabulated function).}$$

#### 6.3.4.2 Full Cox-Munk Model with Gram-Charlier Expansion (CoxMunk)

Let us consider the right-handed system of coordinates (X,Y,Z) centered in the observation point O. Vector OY lies in the principal plane and points in the opposite to the Sun direction, and vector OX is perpendicular to the principal plane. The wave slope (facet) has two components:

$$Z_x = \partial Z / \partial X = \sin \alpha \tan \beta = \frac{\sin \theta \sin \varphi}{\mu + \mu_0}, \quad Z_y = \partial Z / \partial Y = \cos \alpha \tan \beta = \frac{\sin \theta \cos \varphi - \sin \theta_0}{\mu + \mu_0}, \quad (\text{O-3})$$

where  $\alpha$  is the azimuth of ascent (clockwise from the sun), and  $\beta$  is the tilt.

If the distribution of the slope components depends on the wind direction, let us rotate the coordinate system about axis OZ by the angle  $\Delta\varphi_w = \varphi_{wind} - \varphi_0$  clockwise. This gives the new coordinate system (X',Y',Z'), where the axis OY' is aligned with the up-wind direction. In the new coordinates, the slopes (O-3) become:

$$Z_u = Z_{y'} = Z_y \cos \Delta\varphi_w + Z_x \sin \Delta\varphi_w, \quad Z_c = Z_{x'} = -Z_y \sin \Delta\varphi_w + Z_x \cos \Delta\varphi_w, \quad (\text{O-4})$$

and the slope probability density function can now be written as:

$$P(\mu_n) = \frac{1}{2\pi\sigma_u\sigma_c\mu_n^3} \exp\left\{-\frac{\xi^2 + \eta^2}{2}\right\} GC, \quad \eta = Z_u / \sigma_u, \quad \xi = Z_c / \sigma_c. \quad (\text{O-5})$$

The subscripts  $u$  and  $c$  refer to the up-wind and cross-wind components, and the term  $GC$  denotes Gram-Charlier expansion:

$$GC = 1 - 0.5 * C_{21} * (\xi^2 - 1) * \eta - C_{03} / 6 * (\eta^3 - \eta) + C_{40} / 24 * (\xi^4 - 6 * \xi^2 + 3) + C_{22} / 4 * (\xi^2 - 1) * (\eta^2 - 1) + C_{04} / 24 * (\eta^4 - 6 * \eta^2 + 3).$$

The coefficients of expansion are:

$$C_{21} = 0.01 - 0.0086u, \quad C_{03} = 0.04 - 0.033u, \quad C_{40} = 0.4, \quad C_{22} = 0.12, \quad C_{04} = 0.23.$$

In code SHARM, the diffuse reflected radiance is always computed with isotropic NT model, and the direct reflected radiance can be computed with either NT model or the described CoxMunk model. In the last case, the two models are linked by the “energy conservation” condition  $\sigma_U^2 + \sigma_C^2 = \sigma_{NT}^2 = 0.00534u$ . In the experiments, Cox and Munk observed the range of anisotropy  $\sigma_u / \sigma_c = 1-1.8$ , with an average value of 1.34. Currently, SHARM uses  $\sigma_U^2 = 0.6 \sigma_{NT}^2$ ,  $\sigma_C^2 = 0.4 \sigma_{NT}^2$ , so  $\sigma_U / \sigma_C = 1.5$ .

## Code SharmMIE

Code SharmMIE is developed for radiative transfer calculations with aerosols described by MIE scattering theory. It is an integrated package that combines MIE calculations, automatic Legendre expansion of phase function, and RT calculations with code SHARM. It uses the same structure of input data (files “config.par”, “\*.sfc”) with modified input in the file of atmospheric properties “\*.atmMIE”. The results of MIE calculations can be an output as well as the results of code SHARM.

### Main Features:

- Aerosols are represented by polydisperse spherical particles with bi-modal lognormal size distribution or general-form size distribution.
- Aerosol properties (spectral dependence of AOT, single scattering albedo, and phase function) do not change in the vertical but their concentration is variable according to the specified aerosol vertical profile.
- Spectral dependence of aerosol optical characteristics is prescribed by MIE theory (it is not arbitrary).

The other features are the same as for code SHARM-1D. The monodisperse MIE calculations are done with code MIEnoP of W. Wiscombe [1980] translated into C language. The integration over size distribution is performed using Simpson’s quadrature with `_N_Simpson=2001` points. The integration limits are either given by the *min* and *max* radii of the generic-form size distribution, or set to  $r_{\min}=0.05\ \mu\text{m}$  and  $r_{\max}=15\ \mu\text{m}$  for the bi-modal distribution. Parameters `_N_Simpson`,  $r_{\min}$ ,  $r_{\max}$  are specified in the #define statements of the program mieLegRatspl.cpp, and can be changed by an experienced user.

### Run time considerations:

At typical orders of MSH ( $nb=24-48$ ), the run time is almost entirely defined by MIE code, and it is visa versa at high orders of MSH (e.g.  $nb=256$ ). In order to optimize speed of calculations, only  $nb$  coefficients of Legendre expansion that are required for code SHARM are calculated each time.

### Input data:

The configuration file (“config.par”) and the surface properties file (“\*.sfc”) remain the same as for code Sharm-1D. The structure of the atmospheric properties file is changed to accommodate aerosol vertical profile, refractive index and size distribution of aerosol particles.

#### 4.21 Atmospheric Properties File for SharmMIE (\*.atmMIE)

1. szAtmType                      one of 6 Standard Models of the Atmosphere from Lowtran/Modtran: "Tropical", "Midlatitude Summer", "Midlatitude Winter", "Sub-Arctic Summer", "Sub-Arctic Winter", "1976 US Standard". Defines vertical profiles of atmospheric pressure and temperature (file “profile.h”)
2. ib                                  number of layers in atmosphere (starting from the TOA).
3. height[0], ..., height[ib] altitude of boundaries of *ib* layers (in km), e.g. height[0]=100 km (TOA) & height[ib]=0 (BOA).

4. aerProfile[0], ..., aerProfile[ib] relative aerosol profile. For example, aerProfile[0]=0 at TOA, and aerProfile[ib]=1 at (BOA).
5.  $\tau_i^{g-abs}$  [1], ...,  $\tau_i^{g-abs}$  [ib] optical thickness of gaseous absorption on the boundaries of layers (for all wavelengths in separate lines)
6. N\_wavCrefin, wavCrefin[N\_wavCrefin] the number of wavelengths ( $\geq 1$ ) and wavelengths (in  $\mu\text{m}$ ) at which the refractive index is specified  
crefRe[0], ..., crefRe[N\_wavCrefin-1] real part of aerosol refractive index at wavelengths wavCrefin[].  
crefIm[0], ..., crefIm[N\_wavCrefin-1] imaginary part of aerosol refractive index.

(Record 6 provides Real and Imaginary parts of aerosol refractive index at one or more wavelengths (wavCrefin[]). These wavelengths may differ from the wavelengths of RT calculations. In this case, the refractive index is calculated by linear interpolation. Outside of the wavCrefin[] interval of wavelengths, the refractive index is assumed to be constant. If only one wavelength is given, the refractive index is assumed constant in wavelength).

7. szSizeDistr The type of size distribution. Can be either “BiModal” or “SizeDistribution”. In the first case, the size distribution is calculated analytically as bi-modal lognormal model. The user should specify the mean volumetric radius, its standard deviation and concentration for the fine and coarse modes of aerosol. In the second case, the size distribution can be arbitrary. The user should specify the number of particle sizes and then size (radius) and size distribution.

If the size distribution is “BiModal”, then the next record is:

8.  $R_{vf}$ ,  $\sigma_f$ ,  $C_{vf}$  Mean volumetric radius ( $\mu\text{m}$ ), standard deviation ( $\mu\text{m}$ ), and concentration of fine mode,  
 $R_{vc}$ ,  $\sigma_c$ ,  $C_{vc}$  -“- of coarse mode.

If the size distribution is “SizeDistribution”, then the next record is:

8. N\_Radius the number of sizes (particle radii) in the size distribution  
Radius[i],  $i=1, \dots, N\_Radius$  volumetric radius ( $\mu\text{m}$ )  
SizeDistribution[i],  $i=1, \dots, N\_Radius$  size distribution (see AERONET convention, *Dubovik and King*, [2000]).

9. szMiePrint, szPhaseName szMiePrint is a string variable that controls printing of MIE results. If szMiePrint = “PRINT” then the results of MIE calculations and Legendre expansion coefficients are saved in file with provided name (szPhaseName). Otherwise, MIE results are not saved.

...

#### EXAMPLE 1 (for BiModal size distribution)

Line number

(the blue line of text is for explanation only and should NOT be in the file)

```
1976 US Standard (1)
3 (2)
40. 10. 2. 0. (3)
0 0.03 0.25 1. (4)
```

Optical depth of gaseous absorption in three layers for two wavelengths:

```
0.0 0.0 0.0 (for  $\lambda_1$ ) (5)
0.0 0.0 0.0 (for  $\lambda_2$ )
```

Refractive index (from AERONET retrievals):

```
4 0.44 0.67 0.87 1.02 (6)
1.41 1.43 1.465 1.5
```

-0.014 -0.0148 -0.0175 -0.0198

Parameters of size distribution:

BiModal (7)

0.142 0.35 0.035 (8)

3.76 0.73 0.030

PRINT phasel.dat (9)

EXAMPLE 2 (for general-form size distribution)

Line number

1976 US Standard (1)

3 (2)

40. 10. 2. 0. (3)

0 0.01 0.1 1. (4)

Optical depth of gaseous absorption in three layers for two wavelengths:

0.0 0.0 0.0 (for  $\lambda_1$ ) (5)

0.0 0.0 0.0 (for  $\lambda_2$ )

Refractive index (from AERONET retrievals):

4 0.44 0.67 0.87 1.02 (6)

1.41 1.43 1.465 1.5

-0.014 -0.0148 -0.0175 -0.0198

Parameters of size distribution:

SizeDistribution (7)

22 (8)

0.050 0.066 0.086 0.113 0.148 0.194 0.255 0.335 0.439 0.576 0.756 0.992  
1.302 1.708 2.241 2.940 3.857 5.061 6.641 8.713 11.432 15.000

0.001181 0.001437 0.002599 0.005913 0.010309 0.007208 0.002433 0.000916 0.000798

0.001861 0.005347 0.007423 0.005286 0.004878 0.007360 0.010281 0.007811 0.003622

0.001707 0.001128 0.001047 0.001261

PRINT phasel.dat (9)

Two examples of calculations with the “BiModel” and “SizeDistribution” modes are given in the folder Examples. The parameters of the aerosol size distribution were taken from AERONET retrievals over the NASA GSFC.

### Common Error:

If the MIE-part of code gives the error (#...) then the user should check if the input for gaseous absorption optical depth (number of  $\tau$ -values) corresponds to the number of wavelengths specified in “config.par”.

## Code SHARM-3D

Code SHARM-3D was developed for fast and accurate simulations of the monochromatic radiance at the top of the atmosphere over spatially variable surfaces with Lambertian or anisotropic reflectance. The code also calculates the distribution of surface albedo corresponding to given SZA, atmospheric conditions, and BRF distribution. The high speed of calculations is achieved due to:

- parameterization of multiple reflections of light from anisotropic surface;
- use of pre-calculated look-up table of the optical transfer function of the atmosphere;
- explicit parameterization of the solution for TOA radiance in terms of surface BRF parameters by using linear kernel LSRT model for land pixels, and Nakajima-Tanaka model with Lambertian offset for the water pixels.

Like 1D code SHARM, code SHARM-3D performs simultaneous calculations for all specified incidence-view geometries, and multiple wavelengths in one run. The range of view zenith angles is presently limited by the maximal value of  $\mu = -0.3$  in look-up table (LUT) of pre-computed optical transfer function of the atmosphere  $OTF$  ( $\theta \leq 72.5^\circ$ ). Also, the maximal LUT-value of total optical thickness of atmosphere is 0.9. If  $\tau > 0.9$ , we assume that  $OTF(\tau) = OTF(0.9)$ . This assumption has little impact on the accuracy.

The overall description of code SHARM-3D is given in *Lyapustin and Wang* [2005]. This paper was submitted to Applied Optics, and its pdf-file is located in the same folder as this Manual.

### Limitations:

- The atmosphere is laterally uniform across the image. For convenience, it is divided in two vertical layers with aerosols in the bottom layer.
- The surface boundary condition is periodic.
- The code is monochromatic, and does not include polarization.

### Input Data.

The configuration file (“config.par”) and the atmospheric properties file (“\*.atm”) are the same as for 1D code SHARM. However, convention in file “config.par” for the output (parameters szPrint, szRTMode) is slightly different. First, the radiance is calculated and printed only for the top of the atmosphere. SHARM-3D ignores the specified value of parameter szPrint and assigns it the value of “TOA”. Second, parameter szRTMode can only take two values (one for printing radiance only, and another for printing radiance and surface albedo, corresponding to BRF and SZA):

#### 10. Print Mode (file “config.par”)

Two print parameters govern the output of radiance and fluxes:

1. szPrint - specifies interfaces for which results are printed. The results are always printed for the TOA.  
TOA – print for TOA;
2. szRTMode – specifies what to calculate and print. It can be one of two:  
RadOnly – print radiance only;  
FluxRad – prints both radiances and surface albedo.

The format of the surface properties file (“\*.sfc”) is different from code SHARM.

## Surface Properties Files (\*.sfc)

1. szDimRT, chLambert:  
 szDimRT            the dimension of the solution. Takes values of “3D” and “1D”. In the first case, SHARM-3D calculates the full 3D radiance. In the second case it uses Independent Pixel Approximation (IPA), in other words it calculates the 1D radiance separately for each pixel.  
 chLambert            Type of surface reflectance. Takes values of ‘L’ – Lambertian, or ‘A’ – anisotropic.
2. nx\_Image, ny\_Image, resImage  
 (int) nx\_Image, ny\_Image            the x-, y-size of the image. Must be a power of 2!  
 (double) resImage            Spatial resolution of image (size of a pixel) in km.
3. file\_name\_L file\_name\_V file\_name\_GO            The names of files containing the weights of the Lambertian, Volumetric and Geometric-Optical kernels of the LSRT model. The size of the files is nx\_Image×ny\_Image. The rows represent x-axis, and the columns represent y-axis.
4. Wind Speed (m/s), Solar azimuth (in degrees)            Azimuth is counted clockwise from x-axis, which aims at the east direction (Figure 2). The wind speed is required to calculate reflectance from roughened water surface with the model of Nakajima and Tanaka. The wind speed is assumed constant for the whole image. If all of the pixels are land pixels, the wind speed SHOULD be set to zero (this saves the computer time a little).

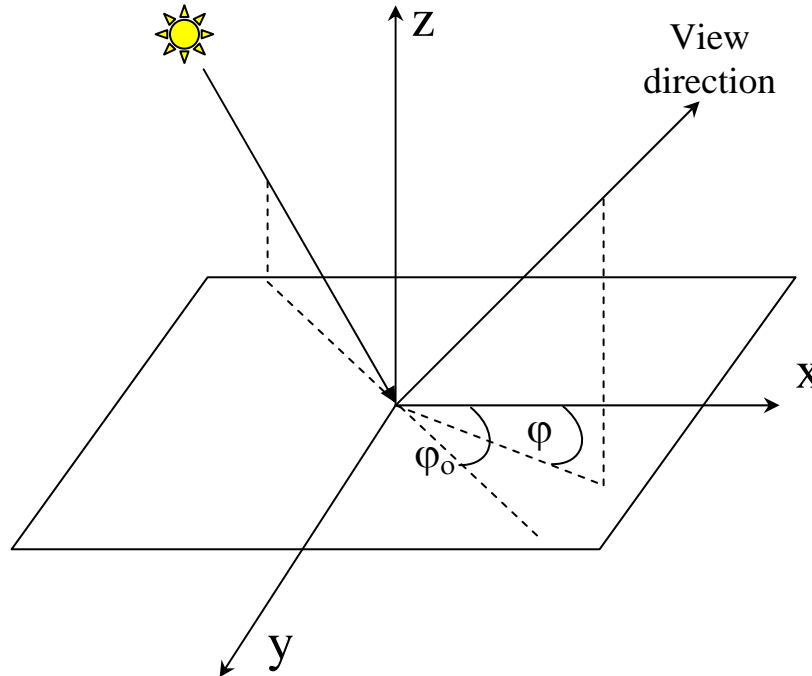


**Figure 2.** Definition of azimuth for 3D calculations.

Example (file “1A.sfc”):

3D A (1)

(3D mode of calculations, anisotropic surface)

32 32 0.5 (2)

(image size is 32 by 32 pixels, spatial resolution is 500 m)

kL\_32.dat kV\_32.dat kGO\_32.dat (3)

5. 45. (4)

(wind speed is 5 m/s, and solar azimuth is 45°)

or

0. 45. (4)

(all pixels are land pixels, and solar azimuth is 45°)

## References:

- Code SHARM (SharmMIE):

Until [Lyapustin, 2005] is published, please use the following reference:

Lyapustin, A. I., and T. Z. Muldashev, Method of spherical harmonics in the radiative transfer problem with non-Lambertian surface, *J. Quant. Spectrosc. Radiat. Transfer*, **61** (4), 545-555, 1999.

- Code SHARM-3D:

Until [Lyapustin and Wang, 2005] is published, please use the following reference:

Lyapustin, A., Radiative transfer code SHARM-3D for radiance simulations over a non-Lambertian nonhomogeneous surface: intercomparison study, *Appl. Optics*, **41**, 5607-5615, 2002.

## REFERENCES

- B. A. Bodhaine, N. B. Wood, E. G. Dutton, J. R. Slusser, "On Rayleigh Optical Depth Calculations," *J. Atmos. Oceanic Technology* **16**, 1854-1861 (1999).
- C. Cox and W. Munk, Measurements of the roughness of the sea surface from photographs of the Sun's glitter, *J. Opt. Society Am.*, **44**, 838-850, 1954.
- Dubovik, O., M. D. King, A flexible inversion algorithm for retrieval of aerosol optical properties from Sun and sky radiance measurements. *J. Geophys. Res.*, **105**, 20,673-20,696, 2000.
- Engelsen, O., B. Pinty, M. M. Verstraete, and J. V. Martonchik, Parametric bidirectional reflectance factor models: Evaluation, improvements and applications, Eur. Rep. 16426 EN, Space Appl. Inst., Ispra, Italy, 1996.
- Gao, F., X. Li, A. Strahler, and C. Schaaf, "Evaluation of the Li Transit kernel for BRF modeling," *Rem. Sens. Reviews* **19**, 205-224 (2000).
- Gordon, H. R., and M. Wang, Surface-roughness considerations for atmospheric correction of ocean color sensors. I: The Rayleigh-scattering component, *Appl. Optics*, **31**, 4247-4260, 1992.
- Hale, G. M., and M. R. Querry, Optical constants of water in the 200-nm to 200  $\mu$ m wavelength region, *Appl. Optics*, **12**, 555-563, 1973.
- Karp, A. H., J. Greenstadt and J. A. Fillmore, *J. Quant. Spectrosc. Radiat. Transfer*, **24**, 391, 1980.
- Lucht W., Schaaf C. B., Strahler A. H., "An algorithm for the retrieval of albedo from space using semiempirical BRDF models," *IEEE Trans. Geosci. Remote Sens.* **38**, 977-998 (2000).
- Lyapustin, A. I., and T. Z. Muldashev, Method of spherical harmonics in the radiative transfer problem with non-Lambertian surface, *J. Quant. Spectrosc. Radiat. Transfer*, **61** (4), 545-555, 1999.
- Lyapustin, A. I., and T. Z. Muldashev, Generalization of Marshak boundary condition for non-Lambert reflection, *J. Quant. Spectrosc. Radiat. Transfer*, **67**, 457-464, 2000.
- Lyapustin, A., Radiative transfer code SHARM-3D for radiance simulations over a non-Lambertian nonhomogeneous surface: intercomparison study, *Appl. Optics*, **41**, 5607-5615, 2002.
- Lyapustin A., Interpolation and Profile Correction (IPC) Method for Shortwave Radiative Transfer in Spectral Intervals of Gaseous Absorption, *J. Atmos. Sci.*, **60**, 865-871, 2003.
- Lyapustin, A. I., "Radiative Transfer Code SHARM for Atmospheric and Terrestrial Applications," *Applied Optics*, submitted (2005).
- Lyapustin, A., and Y. Wang, "Parameterized Code Sharm-3D for Radiative Transfer Over Inhomogeneous Surfaces," *Applied Optics*, submitted (2005).
- Marshak, R. E., Note on the spherical harmonics method as applied to the Milne problem for a sphere, *Phys. Rev.*, **71**, 443-446, 1947.
- Martonchik, J.V., D.J. Diner, B. Pinty, M.M. Verstratete, R.B. Myneni, Yu. Knyazikhin, and H.R. Gordon, 1998. Determination of land and ocean reflective, radiative and biophysical properties using multiangle imaging, *IEEE Trans. Geosci. Remote Sens.*, **36**, 1266-1281.
- Muldashev, T. Z., A. I. Lyapustin, and U. M. Sultangazin, Spherical harmonics method in the problem of radiative transfer in the atmosphere-surface system, *J. Quant. Spectrosc. Radiat. Transfer*, **61** (3), 393-404, 1998.
- Nakajima, T., and M. Tanaka, Effect of wind-generated waves on the transfer of solar radiation in the atmosphere-ocean system, *J. Quant. Spectrosc. Radiat. Transfer*, **29**, 521-537, 1983.

- Nakajima, T., and M. Tanaka, Algorithm for radiative intensity calculations in moderately thick atmospheres using a truncation approximation, *J. Quant. Spectrosc. Radiat. Transfer*, **40**, 51-69, 1988.
- Rahman, H., B. Pinty, and M. M. Verstraete, Coupled surface-atmosphere reflectance (CSAR) model. 2. Semiempirical surface model usable with NOAA advanced very high resolution radiometer data, *J. Geophys. Res.*, **98**, 20,791-20,801, 1993.
- Stamnes, K., S.-C. Tsay, W. Wiscombe and K. Jayaweera, *Appl. Optics*, **27**, 2502, 1988.
- Wiscombe, W., Improved Mie scattering algorithms, *Appl. Opt.*, **19**, 1505-1509, 1980.